Plant Science 321 (2022) 111315

Contents lists available at ScienceDirect

Plant Science

journal homepage: www.elsevier.com/locate/plantsci

Cloning and functional characterization of three sesquiterpene synthase genes from *Chamaecyparis formosensis* Matsumura

Chong-Yao Hong [a], Nai-Wen Tsao [b], Sheng-Yang Wang [b], Fang-Hua Chu [a,*]

[a] School of Forestry and Resource Conservation, National Taiwan University, Taipei, Taiwan
[b] Department of Forestry, National Chung-Hsing University, Taichung, Taiwan

ARTICLE INFO

Keywords:
Sesquiterpene synthase
Gymnosperm
Chamaecyparis formosensis
Biochemical enzyme characterization
Plant specialized metabolites

ABSTRACT

Terpene synthase (TPS) analysis may contribute to a better understanding of terpenoids biosynthesis and the evolution of phylogenetic taxonomy. *Chamaecyparis formosensis* Matsumura is an endemic and valuable conifer of Taiwan. Its excellent wood quality, fragrance, and durability make it become the five precious conifers in Taiwan. In this study, three sesquiterpene synthase genes that belong to the TPS-d2 clade were isolated and characterized through in vitro reaction of recombinant protein and in vivo reaction of *Escherichia coli* heterologous expression system. The main product of Cf-GerA was germacrene A using GC/MS analysis, while the product of Cf-Aco and Cf-Gor were identified as acora-4(14),8-diene and (5*R*,6*R*,10*S*)-α-gorgonene by using NMR analysis. These are the first reported enzymes that biosynthesize acora-4(14),8-diene and (5 *R*,6 *R*,10 *S*)-α-gorgonene. Both sesquiterpene synthases may isomerize the farnesyl pyrophosphate substrate to nerolidyl pyrophosphate for further cyclization. Cf-Aco may catalyze 1,6-cyclization of nerolidyl cation while Cf-Gor may catalyze through an uncharged intermediate, isogermacrene A.

1. Introduction

Terpenoids are the largest group of plant products, and they are also the main component of secondary metabolites synthesis by plants (Gershenzon and Dudareva, 2007; Howe and Jander, 2008). Numerous studies have indicated that terpenoids play an essential role in interaction with other organisms (Sharma et al., 2017). For instance, monoterpenoids and sesquiterpenoids attract parasitoids or predators for indirectly defending against herbivores, and serving as a repellent to larval feeding and oviposition (Sharma et al., 2017). In conifers, once wounded by herbivores, secretion of diterpene resin acids would push the herbivores out or trap herbivores through solidification, sealing the wounds (Keeling and Bohlmann, 2006a). Rice (*Oryza sativa*) also produces an array of diterpenoids, which act as phytoalexin to inhibit spore germination and germ tube elongation of rice blast fungus *Magnaporthe oryzae* (Horie et al., 2015), or serve as allelopathy compound to influence the growth or germination of neighbor plants (Macías et al., 2007). In addition, plant terpenoids could attract pollinators and seed dispersers and even communicate with other plants (Baldwin, 2010; Mithöfer and Boland, 2012). From the utilization point of view, terpenoids are the major composition of plant essential oils, which are widely used as flavouring agents or the natural resources for further isolation of aroma compounds (Caputi and Aprea, 2011). Terpenoids are important sources of phytomedicines, such as artemisinin, a sesquiterpenoid from Artemisia annua, and its derivatives are an essential new anti-malarial class drug (Meshnick, 2002). Terpenoids are also the resources for alternative energy or environment-friendly pesticides. For instance, bisabolane, the fully reduced form of sesquiterpene bisabolene, was an alternative to D2 diesel fuel (McAndrew et al., 2011). On the other hand, the derivate of δ-cadinene, (+)-gossypol, possess the significant postictal activity and anti-fungal activity, and does not show the toxically impact on mammalian animals (Gershenzon and Dudareva, 2007).

Abbreviation: 13C NMR, carbon-13 nuclear magnetic resonance; cTP, chloroplast transit peptide; COSY, 1-1H correlation spectroscopy; DEPT, distortionless enhancement by polarization transfer; FPP, farnesyl pyrophosphate; GC-MS, gas chromatography-mass spectrometry; GPP, geranyl pyrophosphate; GGPP, geranylgeranyl pyrophosphate; HMBC, heteronuclear multiple bond correlation; HSQC, heteronuclear single quantum coherence; IUCN, International Union for Conservation of Nature; IPTG, isopropyl-β-D-thiogalactopyranoside; KI, Kovats retention index; NPP, nerolidyl pyrophosphate; NGS, Next Generation Sequencing; NMR, nuclear magnetic resonance spectroscopy; NOESY, nuclear Overhauser effect spectroscopy; 1H NMR, proton nuclear magnetic resonance; RACE, rapid amplification of cDNA ends; SPME, solid-phase microextraction; TPS, terpene synthase; UTR, untranslated region.

* Corresponding author.
E-mail address: fhchu@ntu.edu.tw (F.-H. Chu).

https://doi.org/10.1016/j.plantsci.2022.111315
Received 22 February 2022; Received in revised form 29 April 2022; Accepted 6 May 2022
Available online 18 May 2022

The precursors of terpenoids are composed of isoprenyl pyrophosphates and dimethylallyl pyrophosphates through the mevalonate pathway to generate C15 farnesyl pyrophosphate (FPP) in the cytosol, or by methyl-erythritol 4-phosphate pathway, generating C10 geranyl pyrophosphate (GPP) or C20 geranylgeranyl pyrophosphate (GGPP) in plastids. Then GPP, FPP, and GGPP will be further eliminated pyrophosphate and cyclized through various terpene synthases (TPSs). Then, derivate terpenoids can be oxidized, ring contracted, or intramolecular cyclized by cytochrome P450 (Keeling and Bohlmann, 2006b; Mizutani and Sato, 2011).

C. formosensis is the endemic precious conifer in Taiwan. It has been recognized as one of the five valuable conifers in Taiwan due to its wood fragrance, fine texture, low dimension heterogeneity, and excellent durability. The compositions of essential oil have shown various effects, such as chamaecynone, 12-hydroxyisointermedenol and 4α-hydroxy-β-methyldihydrocostol. These compounds were active against wood rot fungi (Wang et al., 2005). On the other hand, 1-epi-cubenol, T-cadinol, T-muurolol and α-cadinol have shown excellent antitermitic activity, while T-muurolol and α-cadinol possess outstanding activity against several phytopathegenic fungi (Ho et al., 2012; Hsu et al., 2016). According to International Union for Conservation of Nature (IUCN), *C. formosensis* is an endangered species. Therefore, consuming a large amount of essential oil would cause a more dangerous status for this species. However, it is possible to get valuable terpenoids without destroying *C. formosensis* by expressing TPSs through heterologous expression system. Previously, a monoterpene synthase, Cf-Pin; a sesquiterpene synthase, Cf-Cad, and several diterpene synthases had been identified and characterized (Chu et al., 2009; Kuo et al., 2012; Ma et al., 2021). Three novel sesquiterpene TPSs of *C. formosensis* were reported in this study. The new compounds were verified using NMR analysis, and the proposed cyclization of these TPSs was also illustrated.

2. Materials and methods

2.1. Plant materials and RNA isolation

The needles of 80-year-old *C. formosensis* were obtained from the Chi-Tou Tract of the Experimental Forest of National Taiwan University in 2014 and were identified by Sheng-Yang Wang (Department of Forestry, National Chung-Hsing University). The leaf sample was flash-frozen in liquid nitrogen after collected from plants, then was stored at − 80 °C. First, total RNA was isolated following the method reported in previous research (Chu et al., 2009). Then, the quality of RNA was verified through electrophoresis. Remained RNA was stored at − 80 °C.

2.2. Construction and identification of full-length cDNA clones

With Next-Generation Sequencing (NGS) database (SRA #SRX4056858), which was published in our previous study (Ma et al., 2021), three TPSs were used as bait for the blast. These bait TPSs are abietadiene cyclase (Accession number: AAB05407.1) from *Abies grandis*, LPS (Accession number: AY574248.2) from *Ginkgo biloba,* and Pa-LAS (Accession number: AY473621.1) from *Picea abies*. Most complete sequences were chosen for gene identification because they might have a higher expression level in needle tissue. HiScriptII Reverse Transcriptase (ZGene Biotech, Taipei, Taiwan) was used to synthesize cDNA from total RNA. Rapid amplification of cDNA ends (3′-RACE and 5′-RACE) were carried out with Blend *Taq* (TOYOBO, Osaka, Japan) to obtain the full-length cDNA sequence. Then, with Phanta Super-Fidelity DNA Polymerase (ZGene Biotech, Taipei, Taiwan) and specific primers, as shown in Table S2, the complete open reading frames were amplified with polymerase chain reaction (PCR) and ligated to pGEMT-easy vector (Promega, Madison, WI, USA) for sequencing with ABI PRISM® 3700 DNA Analyzer. The sequences of the genes were then blasted by Translated Basic Local Alignment Search Tool (blastx, http://blast.ncbi.nlm.nih.gov/Blast.cgi) to predict enzyme function by comparing it with similar TPS amino acid sequences.

The translated sequences of three sesquiterpene synthases were then aligned with other sesquiterpene synthases from *T. cryptomerioides* for conserved domain identification (Table S1). TPSs that belong to the TPS-d2 clade. They were used for sequence logos created through Weblogo (https://weblogo.berkeley.edu/logo.cgi). Maximum likelihood method was used to construct the phylogenetic tree with MEGA 7 software with bootstrap value of 500 (Jones et al., 1992; Kumar et al., 2016). Meanwhile, the 3D structure of the enzyme was predicted by using SWISS-MODEL (http://swissmodel.expasy.org) and figures were produced by BIOVIA Discovery Studio Visualizer.

2.3. Heterologous expression of TPSs in E. coli

The full-length *TPSs* gene was cloned into pET28a or pET21a expression vector. The 5′ and 3′-specific primers with restriction endonuclease sites were designed as shown in Table S2.

To examine the expression of *TPSs*, the plasmid was transformed into *E. coli* strand BL21DE3-C41 (Lucigen, Middleton, WI, USA). Cells were grown in 750 ml LB to an OD_{600} of 0.6. After that, 0.4 mM isopropyl-β-D-thiogalactopyranoside (IPTG) was added and incubated at 16 °C for 24 h. Cells were centrifuged at 4 °C, 8400*g* following the former step. Binding buffer (50 mM HEPES & 300 mM NaCl) was used to resuspend the cells, then disrupted by sonication and centrifuged (4 °C, 9300*g*) followed by purifying soluble protein with TALON resin affinity column.

2.4. Enzyme characterization

To characterize the function of the protein with FPP, an assay was carried out in 0.5 ml with 30 μg protein sample in buffer, composed of 250 mM HEPES, pH 7, 1 M KCl, 1 M $MgCl_2$, 10% Glycerol, 0.1 M dithiothreitol and 10 mM Vitamin C, and 11 μl FPP (Sigma, St Louis, MO, USA, 1 mg/ml). The product reacted at 30 °C for 1 h.

2.5. Identification of the product by solid-phase microextraction and GC-MS

The in vitro product was then extracted by using the solid-phase microextraction (SPME) method. The SPME holder and 75 μm carboxen-polydimethylsiloxane were purchased from Supelco (Bellefonte, PA, USA) and performed. After adsorbing for 30 mins, the product was desorbed at gas chromatography-mass spectrometry (GC-MS, TRACE GC Ultra and Polaris Q, Thermo) injection port for 1 min at 250 or 150 °C for compound analysis of Cf-GerA while 250 °C for Cf-Aco and Cf-Gor. DB-5 ms (crossbond 5% phenyl methylpolysiloxane, 30 m * 0.25 mm*0.25 μm) column was used, helium was used as the carrier gas, which has a constant flow rate of 1 ml min^{-1}. For analyzing the product of Cf-GerA, the temperature was 60 °C at first, followed by an increase of 5 °C min^{-1} to 180 °C, then 30 °C min^{-1} to 290 °C and held for 3 mins. To analyze the product of Cf-Aco and Cf-Gor, the temperature was 60 °C at first, followed by an increase of 5 °C min^{-1} to 210 °C, then 30 °C min^{-1} to 250 °C, and then held for 3 mins.

2.6. In vivo co-expression of TPSs in E. coli

The in vivo expression system contained three plasmids, including pMBI (Addgene plasmid #17816), pCOLAduet™ (Novagen, WI, USA) -FPPS, and pET21a-TPSs. The pMBI plasmid contains several upstream genes of the mevalonate pathway, which produce substrates for FPPS from *T. cryptomerioides* (Accession number: MK422457). The pCOLAduet™-FPP plasmid was constructed in previous research (Ma et al., 2019). The FPP substrates were further catalyzed by TPSs. For coexpression, *E. coli* were transformed with the foregoing plasmid and inoculated in 500 ml Super Optimal Broth (SOB) containing 5 μg/ml tetracycline, 15 μg/ml kanamycin, and 25 μg/ml carbenicillin at 37 °C to an OD600 of 0.6. Then, multiple genes were induced by adding IPTG to a

final concentration of 1 mM. To facilitate the terpene synthesis, mevalonolactone (Sigma-Aldrich) was added to a final concentration of 10 mM after the induction. Induction proceed for 72 h and equal volume of n-hexane was added for terpene extraction. Extraction was concentrated through rotary evaporation and analyzed by GC-MS.

2.7. Nuclear magnetic resonance (NMR) analysis

The hexane extracts were concentrated and purified through Strata® Silica-Based Solid Phase Extraction (SPE) column (Phenomenex, CA, USA) with n-hexane. The products were verified and quantitated by GC-MS. For NMR analysis, about 5 mg of purified compounds were dissolved in deuterated chloroform ($CDCl_3$, Sigma-Aldrich). Structure analysis used ^{1}H and ^{13}C spectra with Bruker Avance 400 MHz NMR spectrometer (Bruker, https://www.bruker.com) using TOPSPIN (Bruker).

2.8. Accession numbers

All sequence data have been submitted to the National Center for Biotechnology Information (NCBI) database under accession numbers MG930776 (*Cf-GerA*), MW589642 (*Cf-Aco*) and MW589643 (*Cf-Gor*).

3. Results and discussion

3.1. Cloning of three TPSs

Three *C. formosensis TPSs* (*CfTPSs*) were cloned from cDNA of *C. formosensis*, named *Cf-GerA, Cf-Aco* and *Cf-Gor,* according to the following function identification. *Cf-GerA* has an open reading frame consisting of 1770 bp, while both *Cf-Aco* and *Cf-Gor* have open reading frames composed of 1758 bp. The 5′ untranslated region (UTR) of *Cf-GerA, Cf-Aco* and *Cf-Gor* are 61, 54 and 66 bp, while 3′UTR are 186, 265 and 61 bp. These *TPSs* contain 9 introns and the genomic length of *Cf-GerA* is 3787 bp (Accession number: ON337838), while the genomic length of *Cf-Aco* (Accession number: ON337839) and *Cf-Gor* (Accession number: ON337840) are 2981 bp and 2954 bp. The longer sequence of Cf-GerA was due to a longer intron XIII. By blasting the sequence of three TPSs with blastx, genes with lowest E-value were announced as sesquiterpene synthases, indicating that three TPSs could be sesquiterpene synthase genes. *Cf-Aco* and *Cf-Gor* have a high translated sequence identity of 89.23%, while *Cf-GerA* only has 44.07% and 44.71% translated sequence identity to *Cf-Aco* and *Cf-Gor*, respectively. The alinement of three *TPSs* and two sesquiterpene synthases from *T. cryptomerioides* was shown in Fig. 1a. The amino acid sequences of three TPSs contain several conservative motifs, which are characteristic

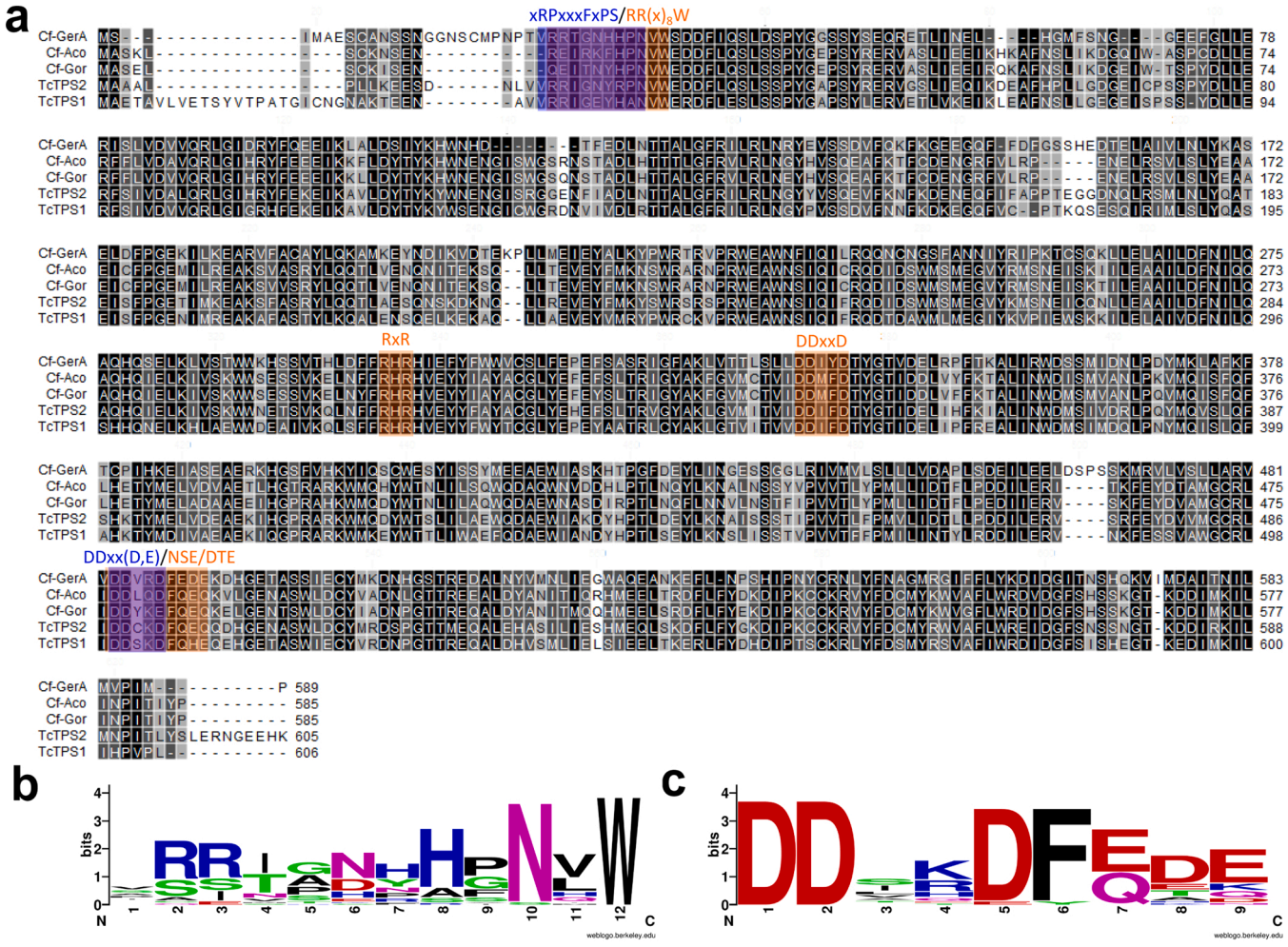

Fig. 1. Alignment of the theoretical amino acid sequence of selected sesquiterpene synthase genes. (a) The conserved motifs of terpene synthase were highlighted with orange ($RR(x)_8W$, RxR, DDxxD and NSE/DTE) or blue (xRPxxxFxPS and DDxx(D/E)). Cf-GerA, Cf-Aco and Cf-Gor, three sesquiterpene synthases characterized from *C. formosensis*. TcTPS1 and TcTPS2 are two sesquiterpene synthases isolated from *T. cryptomerioides*. (b) Sequence logo that focus on the $RR(x)_8W$/ xRPxxxFxPS motif. The amino acid sequences used in this figure are sesquiterpene synthases that originate from gymnosperms in Fig. 6 except GbTPS2, which is lack of $RR(x)_8W$ motif. (c) Sequence logo that focus on the NSE/DTE/DDxx(D/E) motif. The amino acid sequences used in this figure are sesquiterpene synthases that belong to TPS-d2 in Fig. 6.

of terpene synthases. RxR is suggested to prevent the reverse reaction from happening after ionization of the substrates. DDxxD and NSE/DTE are used as substrate binding sites in combination with divalent cations. The RR(x)$_8$W, which is conserved in monoterpene synthase that produces cyclic product, is only conserved in Cf-GerA, while the sequences of Cf-Aco and Cf-Gor were RE(x)$_8$W and QE(x)$_8$W. However, research about δ-cadinene synthase from *G. arboreum* revealed that this motif is essential for active site closure and desolations, which is conserved as xRPxxxFxPS. As for these three enzymes, Cf-GerA is xRRxxxHxPN, Cf-Aco is xRExxxFxPN and Cf-Gor is xQExxxYxPN. As shown in Fig. 1b, it seems that the serine residues substituted asparagine in most gymnosperm sesquiterpene synthases. The serine residue of xRPxxxFxPS is vital to stabilize the structure of TPSs, while in sesquiterpene synthases of gymnosperm, asparagine may take the place of serine except for GbTPS1 from *G. biloba*, which is a serine at this site. It may indicate that the mutation of serine to asparagine had happened in Pinophyta since sesquiterpene synthases from Pinaceae and Cupressaceae shared the same feature. The NSE/DTE motif is conserved as (N,D)D(L,I,V)x(S,T)xxxE; however, the (+)-δ-cadinene synthase (DCS) from *Gossypium arboretum* owns another DDxx(D/E) motif instead of NSE/DTE motif as prenyltransferase does. Fig. 1c demonstrated that most sesquiterpene synthases that belong to TPS-d2have the same feature as DCS, where a second DDxx(D/E) motif substituted the NSE/DTE motif (Degenhardt et al., 2009; Faraldos et al., 2012; González et al., 2016; Jayaramaiah et al., 2016).

3.2. Functional characterization of three TPSs

In vitro enzyme activity was identified through the heterologous expression in *E. coli* (Fig. 2a), while the in vivo enzyme activity was identified by rebuilding the synthesis pathway of sesquiterpene in *E. coli* (Fig. 2b). Both reactions catalyzed FPP into a major sesquiterpene compound. The primary product of Cf-GerA at 250 °C injector temperature was identified as β-elemene through comparison with an authentic standard. However, β-elemene (Fig. 2c) is a cope rearrangement product of germacrene A (Fig. 2d) (de Kraker et al., 1998), which causes the ten-membered ring structure (Fig. 2d) to become a six-membered ring structure (Fig. 2c). Thus, the temperature of the injection port was decreased to 150 °C. An apparent shift of the main peak was observed, and it turns out that the product should be identified as germacrene A. The Kovats retention index (KI) was compared with Adams' research (Adams, 2007).

Both Cf-Aco and Cf-Gor produced one major compound, whether in the in vivo (Fig. 3a) or in vitro system (Fig. 3b). However, the major products were unknown because no authentic standards were comparable. Therefore, the products were synthesized by large-scale production and identified by NMR analysis. Cf-Aco was $C_{15}H_{24}$ by electron ionization mass spectrometry, four degrees of unsaturation. The proton nuclear magnetic resonance (^{1}H NMR), carbon-13 nuclear magnetic resonance (^{13}C NMR) and distortionless enhancement by polarization transfer (DEPT) data (Fig. S1 and S2) showed Cf-Aco has three methyl

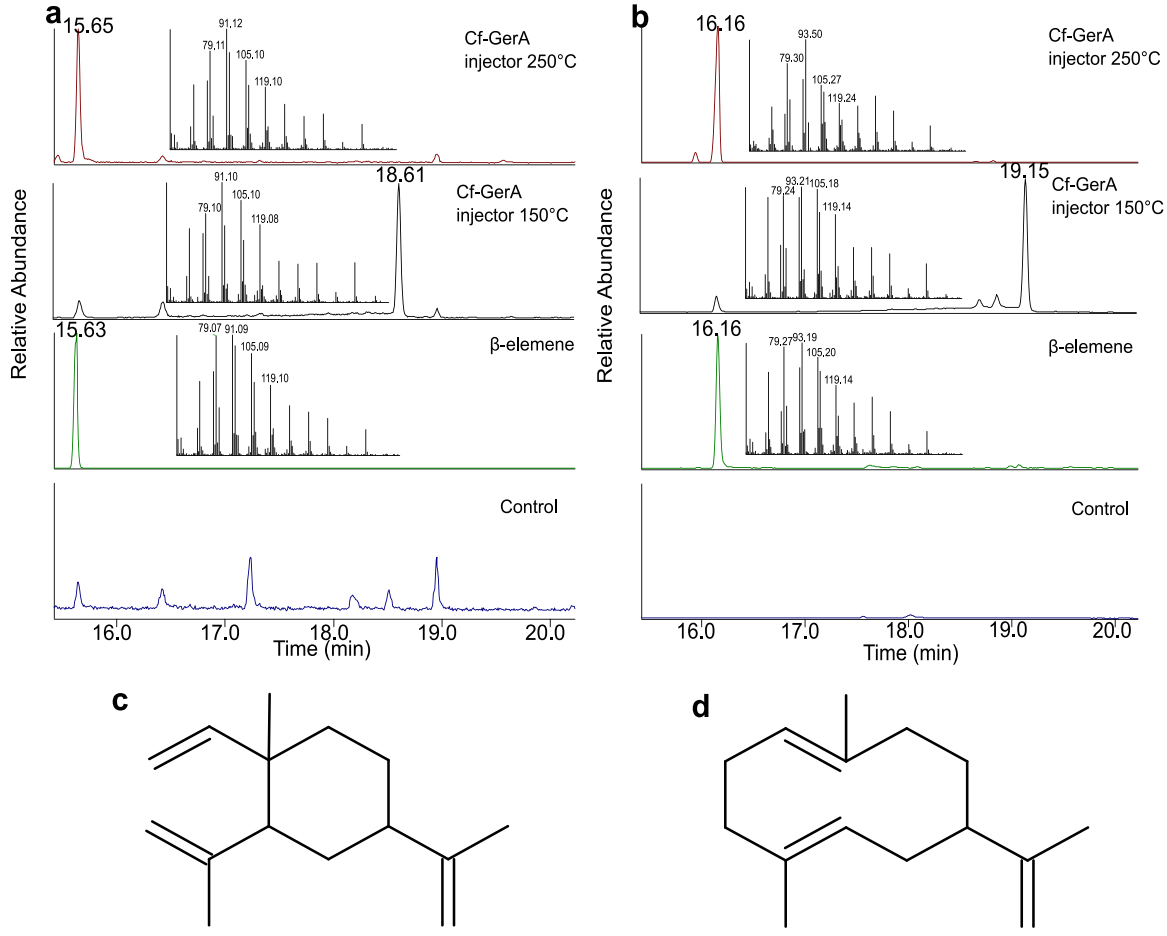

Fig. 2. Enzymatic product analysis of Cf-GerA. Different injection temperatures would lead to different product patterns because the compound is rearranged under higher temperature. (a) The in vitro reaction of Cf-GerA with FPP, different injector temperatures and authentic β-elemene standard are shown. Where temperature of injector was set at 250 °C, The fragments are illustrated and identified as β-elemene while compares to authentic standard. As the temperature of injector was set at 150 °C, the fragments are illustrated and identified as germacrene A. (b) The in vivo reaction of Cf-GerA coexpressed with FPP metabolism pathway rebuilt in *E. coli*, different injector temperature and authentic β-elemene standard are shown. The in vivo reactions produced the same product as in vitro reactions. (c) Molecular structure of β-elemene. d) Molecular structure of germacrene A.

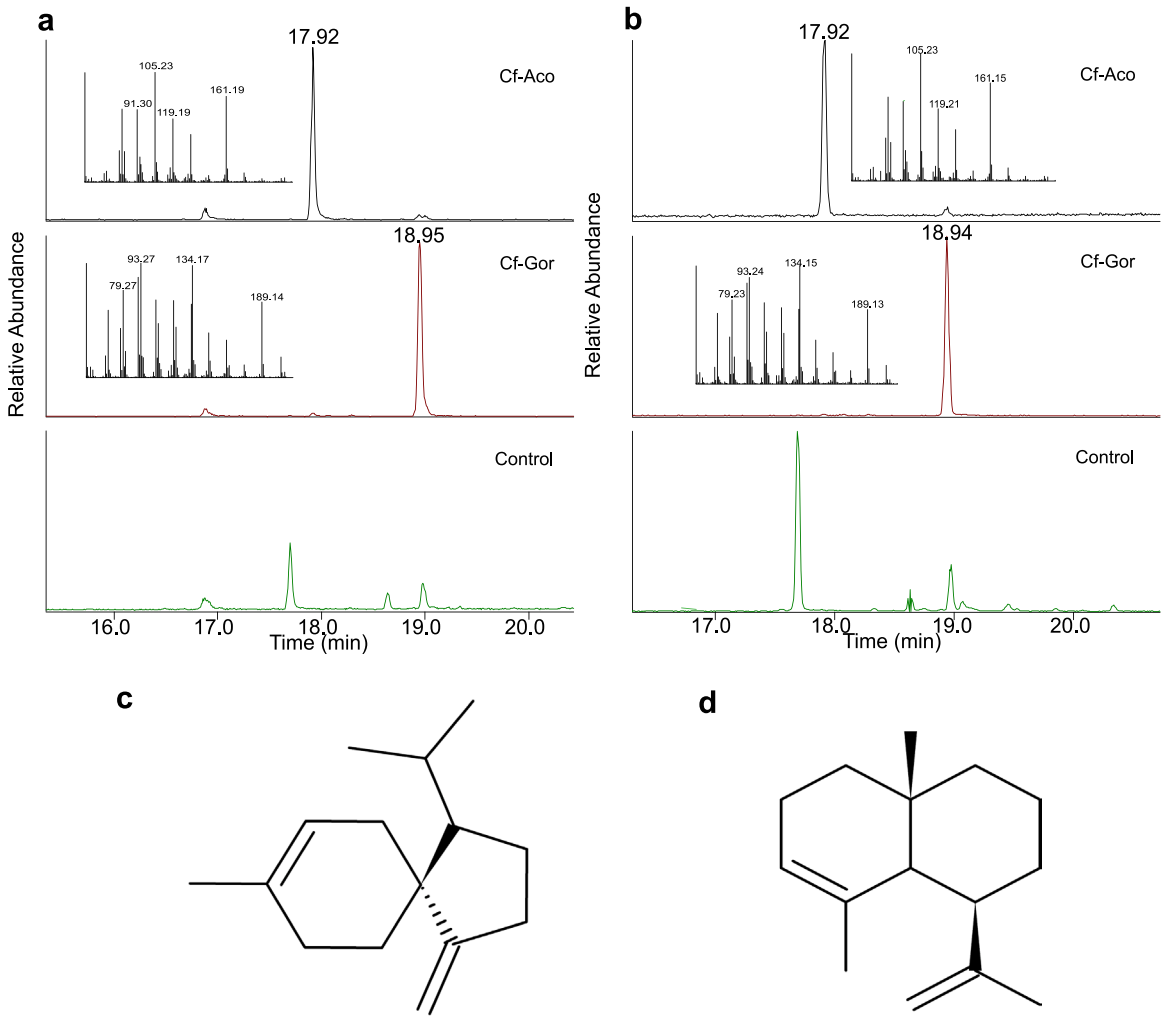

Fig. 3. Enzymatic products analysis of Cf-Aco and Cf-Gor. (a) The in vitro reaction of Cf-Aco and Cf-Gor with FPP substrate, these peaks were not able to compare with any authentic standard, which required NMR for structure elucidation. The peak of Cf-Aco was identified as acora-4(14),8-diene, while the peak of Cf-Gor was identified as (5*R*,6*R*,10*S*)-α-gorgonene through NMR identification. (b) The in vivo reaction of Cf-Aco and Cf-Gor coexpressed with metabolism pathway rebuilt in *E. coli*. The in vivo reactions produced the same product as in vitro reactions. (c) Molecular structure of acora-4(14),8-diene. (d) Molecular structure of (5*R*,6*R*,10*S*)-α-gorgonene.

groups (δ_C 23.5, 20.8, 23.9), one of them attached to a double bond [δ_H 1.62 (br s, 3H, H-15)], the others were isopropyl group [δ_H 0.83, 0.92 (d, J = 6.8 Hz, each 3H, H-12, H-13), 1.74 (m, 1H, H-11)], two double bonds (δ_C 120.5, 133.7, 103.5, 160.6), one of them was trisubstituted olefinic proton [δ_H 5.34 (br s, 1H, H-9)], the others were terminal olefinic protons [δ_H 0.74, 0.74 (dd, J = 3.8, 2.2 Hz, each 1H, H-14)], which was cyclopentane methylidene, five secondary carbons, two tertiary carbons, and one quaternary carbon. The Cf-Aco structure was deduced acorane type skeleton and assigned the position of carbons (Table 1) on the basis of heteronuclear single quantum coherence (HSQC), heteronuclear multiple bond correlation (HMBC), ^{1}H–^{1}H correlation spectroscopy (COSY) and nuclear Overhauser effect spectroscopy (NOESY). The Cf-Aco was identified as acora-4(14),8-diene (Fig. 3c) (Castro et al., 1984; Kuo and Shiu, 1996).

Cf-Gor had the molecular formula $C_{15}H_{24}$ base on electron ionization mass spectrometry, which was four degrees of unsaturation. The Cf-Gor had a methyl group [δ_H 0.79 (s, 3H, H-14)], two methyl groups attached to the double bond [δ_H 1.68 (s, 3H, H-13) and δ_H 1.72 (s, 3H, H-15)], an trisubstituted olefinic proton [δ_H 5.36 (br d, J = 8.4 Hz, 1H, H-3)], two terminal olefinic protons [δ_H 4.68 (d, J = 2.2 Hz, 1H, H-12), 4.75 (dd, J = 2.5, 1.3 Hz, 1H, H-12)] as deduced from the ^{1}H NMR data (Fig. S3). The ^{13}C NMR data of Cf-Gor showed that it contained three methyl groups (δ_C 19.3, 23.1, 27.6), a trisubstituted olefin (δ_C 122.7, 138.8), a terminal olefin (δ_C 112.6, 148.1), five secondary carbons, two tertiary carbons, and one quaternary carbon, based on a DEPT experiment (Fig. S4). From HSQC and HMBC experiments, the proton and carbon correlation of Cf-Gor could be assigned in Table 2. Based on the above evidence, Cf-Gor was a dicyclic sesquiterpene containing an endocyclic double bond, and the structure was similar to α-gorgonene (Hackl et al., 2004). However, the NOESY spectra correlation between H-5, H-13, H-14 suggested that Cf-Gor was the stetrochemistry different from α-gorgonene, and named (5 *R*,6 *R*,10 *S*)-α-gorgonene (Fig. 3d). This is the first report of acora-4(14),8-diene and (5 *R*,6 *R*,10 *S*)-α-gorgonene synthases. However, both compounds have never been identified in the essential oil of *C. formosensis* (Wang et al., 2005; Lin et al., 1999; Su et al., 2006), and further modification by P450 to rare uncharacterized compounds may be possible.

Some of the terpene synthases could catalyze both GPP and FPP. For instance, two terpene synthases, AmNES/LIS-1 and AmNES/LIS-2, both originate from *Antirrhinum majus* are able to convert GPP to linalool and FPP to nerolidol (Nagegowda et al., 2008). Another example is that several sesquiterpene synthases from *T. cryptomerioides* are capable of catalyzing both GPP and FPP (Ma et al., 2019). To find out whether these TPSs can react with GPP or not, GPP was also used as a substrate for in

Table 1
^{1}H and ^{13}C data for product of Cf-Aco ($CDCl_3$, δ in ppm).

Position	δ_C	δ_H
1	53.9	1.45 m
2	24.9	1.42 m
		1.48 m
3	30.3	2.30 m
		2.36 m
4	160.6	–
5	46.3	–
6	23.9	1.45 m
		1.74 m
7	27.4	1.21 m
		1.93 m
8	133.7	–
9	120.5	5.34 br s
10	36.6	1.71 m
		2.30 m
11	27.8	1.74 m
12	20.8	0.83 d (6.8)[a]
13	23.9	0.92 d (6.8)
14	103.5	4.70 dd (3.8, 2.2)
		4.74 dd (3.8, 2.2)
15	23.5	1.62 br s

[a] Coupling constants in Hz.

Table 2
^{1}H and ^{13}C data for product of Cf-Gor. (400 mHz, $CDCl_3$, δ ppm).

Position	δ_C, type	δ_H (*J* in Hz)
1	50.4, CH	2.93 dt (11.5, 9.0)
2	28.3, CH_2	1.21 m
3	23.1, CH_2	1.21 m
		1.48 m
4	35.4, CH_2	2.00 m
4a	42.6, C	–
5	42.0, CH_2	1.26 m
		1.35 td (12.0, 8.1)
6	42.5, CH_2	1.82 m
		2.07 m
7	122.7, CH	5.36 br d (8.4)
		1.60 td (3.4, 14.4)
8	138.8, C	–
8a	56.8, CH	1.76 m
9	148.1, C	–
10	112.6, CH_2	4.68 d (2.2)
		4.75 dd (2.5, 1.3)
11	23.1, CH_3	1.68 s
12	19.3, CH_3	0.79 s
13	27.6, CH_3	1.72 s

vitro reaction. Cf-GerA produced two main products with GPP, which are nerol and geraniol, compared with the authentic nerol and geraniol (Fig. S5). Both Cf-Aco and Cf-Gor produced the same products, and the major compound is α-terpineol (Fig. S6).

From the blast result of three *TPSs*, these TPSs can be characterized as sesquiterpene synthases. Furthermore, according to the prediction of ChloroP 1.1 (http://www.cbs.dtu.dk/services/ChloroP/), a chloroplast transit peptide (cTP) prediction website, these TPSs were predicted to be without cTP, and this is a trait of sesquiterpene synthase (Chen et al., 2011). Therefore, from the evidence above, we speculated that *Cf-GerA*, *Cf-Aco* and *Cf-Gor* could be characterized as sesquiterpene synthase genes.

Sesquiterpene synthases with the ability to isomerize the C2C3 double bonds often produce cyclic compounds with GPP. From the results above, we can postulate that Cf-GerA may not pass through the formation of nerolidyl cation, while Cf-Aco and Cf-Gor may isomerize the FPP substrate to NPP, which is then ionized to nerolidyl cation (Faraldos et al., 2012).

3.3. Reaction Mechanism of Three TPSs

The 3D structure of three TPSs was built through SWISS-MODEL based on an α-bisabolene synthase, AgBIS from *A. grandis* (SWISS-MODEL Template Library ID 3sae.1[9]). Though AgBIS is a sesquiterpene synthase with a three-domain structure, the model of three *TPSs* only shows α and β domain structures consisting of several α-helix secondary structures. The residues that are important for conserved motifs and residues that may have the critical function of cyclization are shown in Fig. 4a–c. Residues may be crucial for the difference of product between Cf-Aco and Cf-Gor are aligned in Fig. 4d. From the amino acid sequence of Cf-GerA, which produced germacrene A as the main product. This compound has a simple cyclization mechanism, which forms from 1,10-cyclization of FPP without isomerizes to nerolidyl pyrophosphate (NPP). The π electrons attack carbocation center, followed by deprotonation and formation of germacrene A (Gonzalez et al., 2014). Some specific residues are responsible for 1,10-cyclization. One of them is A^{479}, which is near the second DDxx(D/E) motif. The alanine residue is shared among germacrene/caryophyllene synthase in *Vitis vinifera*, for instance, VvshirazTPS07; while some sesquiterpene synthases like VvshirazTPS26 from *V. vinifera* are cysteine and hinders the formation of the (*E*, *E*)-germacrenyl cation (Dueholm et al., 2019). Another one is a three amino acid motif, $S^{438}G^{439}G^{440}$. In 5-epi-aristolochene synthase, TEAS of *Nicotiana benthamiana*, the motif amino acid sequence is the triad of threonine residue, which was proposed to play an essential role in the cyclization of farnesyl cation (Starks et al., 1997). However, for gemacrene A synthase from *Solidago canadensis*, GAS, this motif is $T^{401}G^{402}G^{403}$, similar to Cf-GerA. Once the G^{402} residue was substituted with alanine or serine, the 1,11-cyclization activity increased, which caused the accumulation of α-humulene (Gonzalez et al., 2014; Dueholm et al., 2019). Y^{520} from TEAS, the equivalent residue of Y^{561} from Cf-GerA, was involved in the reprotonation of intermediate germacrene A (Starks et al., 1997; Rising et al., 2000). However, this residue may not be involved in reprotonation in Cf-GerA because the cyclization mechanism of germacrene A does not pass through reprotonation of intermediate compound. From the information mentioned above, Cf-GerA might have had the ability of 1,10-cyclization of FPP.

A possible biosynthetic route to Cf-Aco is present in Fig. 5. The pathway starts with the isomerization of FPP and leads to the formation of NPP, and it is plausible structures of most cyclic sesquiterpenoids by suitable cyclization. Bisabolyl cation is formed by 1,6-cyclisation from the tail end of NPP is triggered by ionization of the pyrophosphate moiety and attack from π-electron cloud, subsequent homobisabolyl cation is produced via 1,2-hydride shift. Further 6,10-cyclisation yields the spiro-ring system, which is acorenyl cation, followed by the homo acorenyl cation via 1,2-hydride shift. After that, the 1,4-hydride shift and deprotonation result in the final product, acora-4(14),8-diene. The postulated catalyzing mechanism of Cf-Aco goes through 1,6-cyclization. This cyclization is performed by a critical residue, T^{296} in amorpha-4,11-diene synthase from *Artemisia annua*, ADS (Abdallah et al., 2016), corresponding to T^{333} in Cf-Aco (Fig. 4d). This residue is conserved in other TPSs from *T. cryptomeroides* which catalyzed 1, 6-cyclization, indicating the possibility of forming bisabolyl cation (Ma et al., 2019). On the other hand, one of the residues involved in the 1,10-cyclization, which follows 1,6-cyclization, is G^{439} in ADS. This residue corresponds to C^{473} in Cf-Aco. In ADS, mutation G439C reduced the second 1,10-cyclization and produced more 1,6-cyclization compounds. On the other hand, TcTPS1 is C^{496} at this site, mainly producing zingiberene, a 1,6-cyclization product without secondary cyclization. However, it seems that Cf-Aco was not affected by the C^{473} residue and was still able to perform secondary cyclization, it is possible that other residues may involve in the second 6,10-cyclization of Cf-Aco (Ma et al., 2019; Abdallah et al., 2016).

The product of Cf-Gor contains an isopropyl group at the C6 position, which is also the stereoisomer of α-gorgonene. Sesquiterpenes with the isopropyl group at this carbon are assumed to pass through an

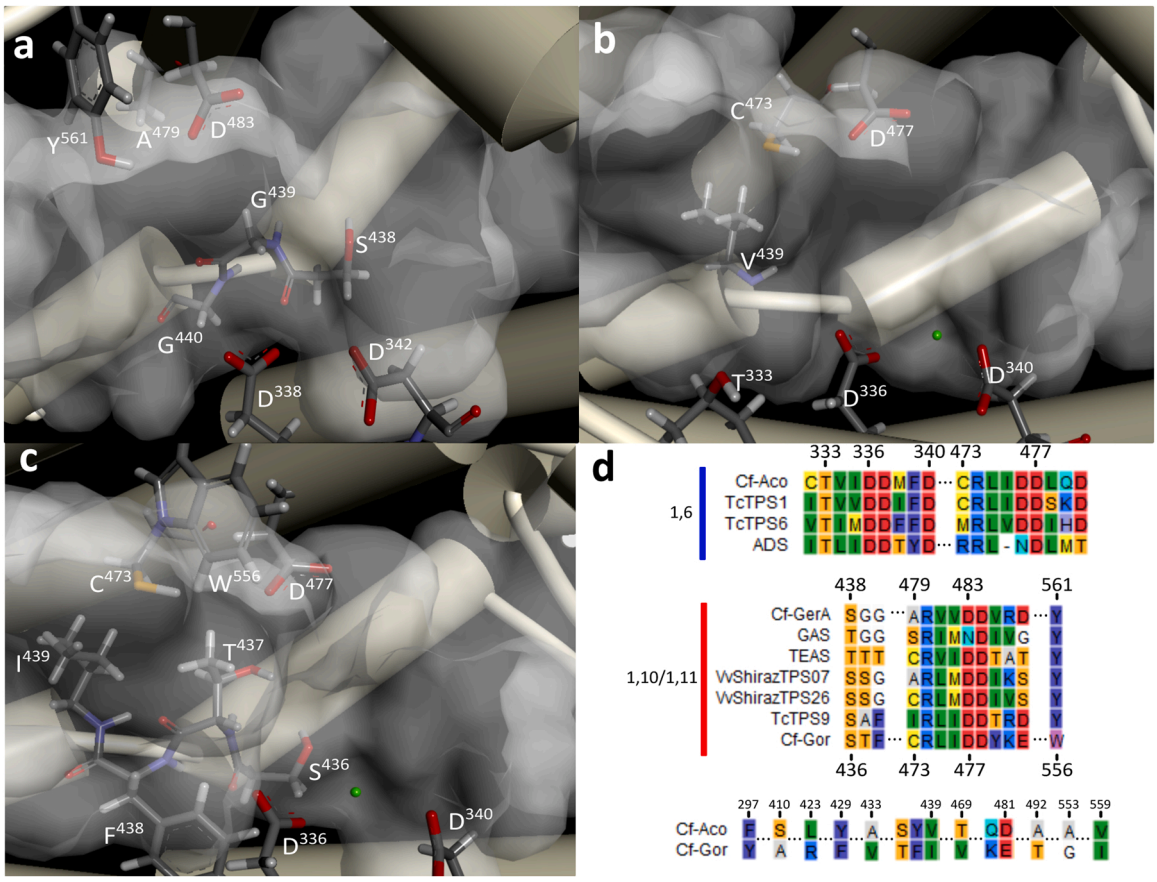

Fig. 4. Predicted 3-D structure of three TPSs. The residues of two aspartate-rich motifs involved in the binding of magnesium ions are illustrated with side chains. Residues that may be involved in the reaction are also illustrated, which are near the predicted active cavity (white region) of TPSs. (a) Residues that might involve in the reaction of Cf-GerA. (b) Residues that might involve in the reaction of Cf-Aco. (c) Residues that might involve in the reaction of Cf-Gor. (d) Alignment of residues involved in the cyclization of FPP and the residues that might cause the different cyclization mechanisms between Cf-Aco and Cf-Gor.

uncharged intermediate, isogermacrene A, which is supposed to be catalyzed from bicyclogermacrene (Hackl et al., 2004). Based on the GPP catalyzed result and the C^{473} residue, which is a residue that corresponds to A^{479} of Cf-GerA, it is possible that the FPP substrate will firstly be isomerized to nerolidyl cation instead of forming the (*E*, *E*)-germacrenyl cation. C^{473} in Cf-Gor is also corresponded to S^{442} in GAS (Fig. 4d). The mutation of S442C caused the formation of more 1, 11-cyclization compounds, which indicates that this residue is related to 1,10 and 1,11-cyclization (Gonzalez et al., 2014; Dueholm et al., 2019). Thus, the nerolidyl cation undergoes an intermediate cation, which may be an intermediate in both 1,10 and 1,11-cyclization catalyzed enzymes. After deprotonation, bicyclogermacrene is formed, which is then followed by protonation and results in the shift of isopropyl group. Deprotonation leads to the formation of isogermacrene A, which is then protonated and via 2,7-cyclization to form gogornenyl cation with deprotonation to the final product as shown in Fig. 5. As discussed above, the mutation of G402A/S of three amino acid motif from GAS cause the elevation of 1,11-cyclization activity. This may result from the common intermediate of 1,10 and 1,11-cyclization, as the second residue mutants to alanine or serine with larger van der Waals volume, and the intermediate is not able to stably perform 1, 10-cyclization (Gonzalez et al., 2014). The three amino acids motif of Cf-Gor is $S^{436}T^{437}F^{438}$ (Fig. 4d). It is supposed that the reaction may pass through the common intermediate cation, while a bigger volume of T^{437} may not cause 1,10-cyclization stably and lead to stable bicyclogermacrene. Intriguingly, the third residue of this three amino acid motif of Cf-Gor is bulky residues, F^{438}, which are smaller glycine of most 1, 11-cyclization TPS in previous research (Gonzalez et al., 2014; Dueholm et al., 2019). In the identified sesquiterpene synthase of *T. cryptomerioides*, TcTPS9 (caryophyllene synthase) is the only enzyme with bulky residue at this site, which has 1,11-cyclization activity (Ma et al., 2019). It is worthy of further research on these residues in the role of 1,10/1,11-cyclization of TPS. As mentioned above, Y^{520} residue of TEAS participates in the protonation of intermediate compounds together with D^{444} and D^{525}. However, Cf-Gor is W^{556} at this site. This residue is known that once the Y520F mutation occurred in TEAS, the protonation of the intermediate would be ceased, and germacrene A was the main product (Dueholm et al., 2019; Starks et al., 1997). Thus, it is speculated that Cf-Gor might protonate their intermediate compounds with tryptophan. However, in order to fully understand the catalyzation mechanism of this TPS, further research is still required.

Although Cf-Aco and Cf-Gor have high sequence identity, their product may go through different cyclization mechanisms. Cf-Aco is speculated to perform 1,6-cyclization while the substrate of Cf-Gor probably goes through 1,10/1,11-cyclization. In previous research, the M447H mutation caused the alternation of the products. The distribution of two 1,10-cyclization products, sibirene and α-ylangene was shown to decrease, while the distribution of 1,6-cyclization product, β-bisabolene increased from 3.3% to 48.3%. The corresponding residue of M^{447} in *A. grandis* γ-humulene synthase is V^{439} and I^{439} in Cf-Aco and Cf-Gor, respectively, are V^{439} and I^{439}. Although they are both nonpolar residues, it can't be ruled out that this position is vital for the divergence of the cyclization pathway of Cf-Aco and Cf-Gor (Yoshikuni et al., 2006). Besides the residue mentioned above, several differences between the sequence of two TPSs are shown in Fig. 4d. Residues that point to or beside the active cavity are selected for alignment. These residues might

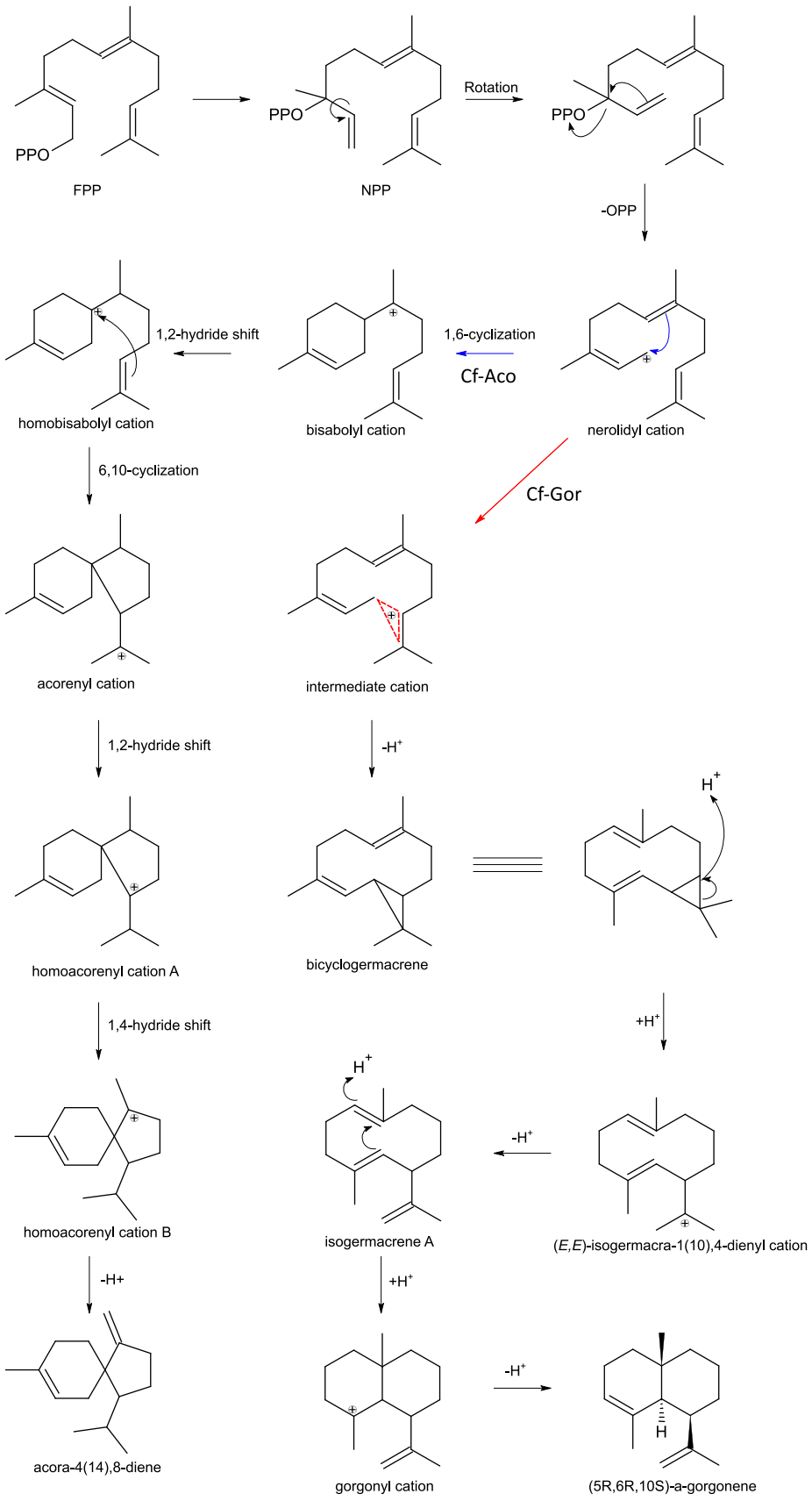

Fig. 5. Proposed cyclization mechanism of Cf-Aco and Cf-Gor. The blue and red arrows indicate the different cyclization pathways of Cf-Aco and Cf-Gor.

be necessary for cyclization, and further experiments that focus on these residues might help us understand the cyclization mechanism of these two TPSs.

3.4. Phylogenetic analysis

The phylogenetic tree was constructed with several amino acid sequence data from NCBI. Three TPSs were placed into the TPS-d2 clade, which contains primarily gymnosperm sesquiterpene synthases (Chen et al., 2011) (Fig. 6).

TPS-d is composed of terpene synthases from gymnosperms, which can be further divided into three groups that are TPS-d1, TPS-d2 and TPS-d3. TPS-d1 is mainly made up of monoterpene synthases and some sesquiterpene synthases, for instance, farnesene synthases, of gymnosperms, while TPS-d2 is composed of other sesquiterpene synthases. TPS-d3 is mainly composed of diterpene synthases, with some exceptions of sesquiterpene synthases (Martin et al., 2004). In the TPS-d2 clade, *Cf-Aco* and *Cf-Gor* are homologous to each other. We can see that TPSs identified in this research are more phylogenetically related to TPSs from *T. cryptomeroides*, which is also a Cupressaceae species, than from other Pinaceae. Because plants have to synthesize a variety of compounds, including terpenoids, in order to accommodate their selves to the environment, which leads to the divergence evolution of TPSs. Therefore, TPSs from the same species will cluster in phylogenetic trees. However, Fig. 6 demonstrated that TPSs from different species with related functions would be clustered together. For instance, Cf-Aco, a 1, 6-cyclization TPS, clustered with TcTPS1 and TcTPS2 of 1,6-cyclization enzymes. While Cf-GerA, a 1,10-cyclization enzyme, clustered with TcTPS3 and TcTPS4, which wereδ-cadinene synthase and germacrene-4-ol synthase catalyzed 1,10-cyclization of FPP substrate.

Also, convergent evolution may happen and cause some TPSs in different species to share the same activity; for instance, both TPS23 from *Zea mays* and TcTPS9 from *Taiwania cryptomerioides* are able to convert FPP into β-caryophyllene. In Fig. 6, even though Cf-GerA and other germacrene A synthases that originated from Asteraceae species (LTC1 and CiGAS) produce the same product, their phylogenetic distances are farther than those originated from gymnosperms. Those two germacrene A synthases from *Asteraceae* species belong to TPS-a, which are mainly composed of sesquiterpene synthases of angiosperm (Ma et al., 2019; Pichersky and Lewinsohn, 2011; Köllner et al., 2008).

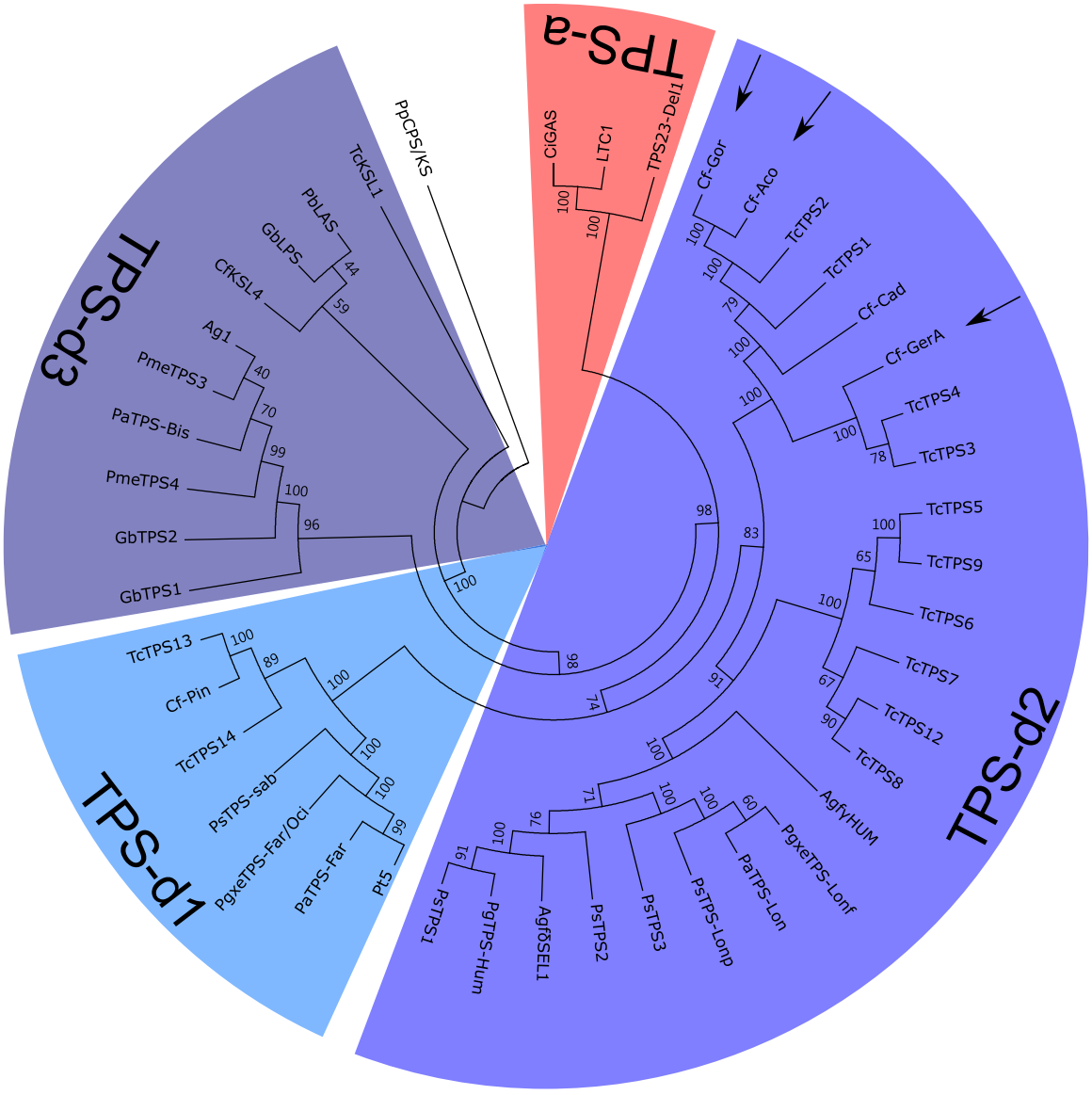

Fig. 6. Phylogenetic tree of several plant terpene synthase amino acid sequences from NCBI. Accession numbers are shown in Table S1. The phylogenetic tree was constructed with MEGA 7 software using the maximum likelihood method.

In Fig. 6, it also revealed that the specificity of terpene synthases is hard to predict on the basis of phylogenetic relationship, resulting from the rapid evolution of TPS sequences through duplication or mutagenesis (Chen et al., 2011). This can be seen from Cf-Gor, which clustered with 1,6-cyclization enzymes but executed 1,10/1,11-cyclization. It is worthy of note that Cf-Aco and Cf-GerA may be a transitional state for sesquiterpene evolution in gymnosperm as proposed by Liang et al. (2021) because they cluster with TcTPS1–4. The research suspects that sesquiterpene synthases from gymnosperm will evolve from acyclic to small ring structures and eventually to large ring structures, and TcTPS1–4 are the transitional states of the functional evolution. On the other hand, Cf-Gor, which might have 1,10/1,11-cyclization ability, was clustered with those 1,6-cyclization enzymes. This indicated that 1, 6-cyclization enzymes were possible to gain the activity of 1,10/1, 11-cyclization during evolution in Cupressaceae.

4. Conclusions

In this research, we identified and characterized three sesquiterpene synthases from the precious conifer, *Chamaecyparis formosensis*, in Taiwan. These enzymes catalyzed FPP into different sesquiterpene compounds: Cf-GerA catalyzed the formation of germacrene A, Cf-Aco catalyzed the formation of acora-4(14),8-diene while Cf-Gor catalyzed the formation of (5*R*,6*R*,10*S*)-α-gorgonene. The enzymes that catalyzed the biosynthesis of acora-4(14),8-diene and (5*R*,6*R*,10*S*)-α-gorgonene are firstly reported. Although Cf-Aco and Cf-Gor have high amino acids sequence identity, they might have different cyclization mechanisms, leading to the distinctive outcome of the product. It is worthy of further research to understand the cyclization mechanism of these two enzymes and find the residues that cause the different outcomes of products.

Funding

This study was funded by the Ministry of Science and Technology, Taiwan. (MOST 110-2313-B-002-039-MY3).

Declaration of Competing Interest

The authors declare that they have no known competing financial interests or personal relationships that could have appeared to influence the work reported in this paper.

Acknowledgments

The authors thank the DNA Sequencing Core Facility (Core Facility and Innovative Instrument Project, AS-CFII-108-115) for DNA Sequencing support. We also gratefully acknowledge the financial assistance provided by the Ministry of Science and Technology, Taiwan [MOST 110-2313-B-002-039-MY3].

Appendix A. Supporting information

Supplementary data associated with this article can be found in the online version at doi:10.1016/j.plantsci.2022.111315.

References

I.I. Abdallah, M. Czepnik, R. van Merkerk, W.J. Quax, Insights into the three-dimensional structure of amorpha-4,11-diene synthase and probing of plasticity residues, J. Nat. Prod. 79 (2016) 2455–2463, https://doi.org/10.1021/acs.jnatprod.6b00236.

R. Adams. Identification of Essential Oil Components By Gas Chromatography/ Mass Spectrometry, 4th ed., Allured Publ., Carol Stream, 2007.

I.T. Baldwin, Plant volatiles, Curr. Biol. 20 (2010) R392–R397, https://doi.org/10.1016/j.cub.2010.02.052.

L. Caputi, E. Aprea, Use of terpenoids as natural flavouring compounds in food industry, Recent Pat. Food Nutr. Agric. 3 (2011) 9–16, https://doi.org/10.2174/2212798411103010009.

V. Castro, J. Jakupovic, F. Bohlmann, A new type of sesquiterpene and acorane derivative from *Calea prunifolia*, J. Nat. Prod. 47 (1984) 802–808, https://doi.org/10.1021/np50035a008.

F. Chen, D. Tholl, J. Bohlmann, E. Pichersky, The family of terpene synthases in plants: a mid-size family of genes for specialized metabolism that is highly diversified throughout the kingdom, Plant J. 66 (2011) 212–229, https://doi.org/10.1111/j.1365-313X.2011.04520.x.

F.-H. Chu, P.-M. Kuo, Y.-R. Chen, S.-Y. Wang, Cloning and characterization of α-pinene synthase from *Chamaecyparis formosensis* Matsum, Holzforschung 63 (2009) 69–74, https://doi.org/10.1515/HF.2009.019.

J. Degenhardt, T.G. Köllner, J. Gershenzon, Monoterpene and sesquiterpene synthases and the origin of terpene skeletal diversity in plants, Phytochemistry 70 (2009) 1621–1637, https://doi.org/10.1016/j.phytochem.2009.07.030.

B. Dueholm, D.P. Drew, C. Sweetman, H.T. Simonsen, In planta and in silico characterization of five sesquiterpene synthases from *Vitis vinifera* (cv. Shiraz) berries, Planta 249 (2019) 59–70, https://doi.org/10.1007/s00425-018-2986-7.

J.A. Faraldos, D.J. Miller, V. González, Z. Yoosuf-Aly, O. Cascón, A. Li, R.K. Allemann, A 1,6-ring closure mechanism for (+)-δ-cadinene synthase? J. Am. Chem. Soc. 134 (2012) 5900–5908, https://doi.org/10.1021/ja211820p.

J. Gershenzon, N. Dudareva, The function of terpene natural products in the natural world, Nat. Chem. Biol. 3 (2007) 408–414, https://doi.org/10.1038/nchembio.2007.5.

V. Gonzalez, S. Touchet, D.J. Grundy, J.A. Faraldos, R.K. Allemann, Evolutionary and mechanistic insights from the reconstruction of α-humulene synthases from a modern (+)-germacrene A synthase, J. Am. Chem. Soc. 136 (2014) 14505–14512, https://doi.org/10.1021/ja5066366.

V. González, D.J. Grundy, J.A. Faraldos, R.K. Allemann, The amino-terminal segment in the β-domain of δ-cadinene synthase is essential for catalysis, Org. Biomol. Chem. 14 (2016) 7451–7454, https://doi.org/10.1039/C6OB01398H.

T. Hackl, W.A. König, H. Muhle, Isogermacrene A, a proposed intermediate in sesquiterpene biosynthesis, Phytochemistry 65 (2004) 2261–2275, https://doi.org/10.1016/j.phytochem.2004.05.024.

C.-L. Ho, K.-F. Hua, K.-P. Hsu, E.I.-chen Wang, Y.-C. Su, Composition and antipathogenic activities of the twig essential oil of *Chamaecyparis formosensis* from Taiwan, Nat. Prod. Commun. 7 (2012) 933–936.

K. Horie, Y. Inoue, M. Sakai, Q. Yao, Y. Tanimoto, J. Koga, H. Toshima, M. Hasegawa, Identification of UV-induced diterpenes including a new diterpene phytoalexin, phytocassane F, from rice leaves by complementary GC/MS and LC/MS approaches, J. Agric. Food Chem. 63 (2015) 4050–4059, https://doi.org/10.1021/acs.jafc.5b00785.

G.A. Howe, G. Jander, Plant immunity to insect herbivores, Annu. Rev. Plant Biol. 59 (2008) 41–66, https://doi.org/10.1146/annurev.arplant.59.032607.092825.

C.-Y. Hsu, C.-Y. Lin, S.-T. Chang, Antitermitic activities of wood essential oil and its constituents from *Chamaecyparis formosensis*, Wood Sci. Technol. 50 (2016) 663–676, https://doi.org/10.1007/s00226-016-0811-7.

R.H. Jayaramaiah, A. Anand, S.D. Beedkar, B.B. Dholakia, S.A. Punekar, R.M. Kalunke, W.N. Gade, H.V. Thulasiram, A.P. Giri, Functional characterization and transient expression manipulation of a new sesquiterpene synthase involved in β-caryophyllene accumulation in *Ocimum*, Biochem. Biophys. Res. Commun. 473 (2016) 265–271, https://doi.org/10.1016/j.bbrc.2016.03.090.

D.T. Jones, W.R. Taylor, J.M. Thornton, The rapid generation of mutation data matrices from protein sequences, Bioinformatics 8 (1992) 275–282, https://doi.org/10.1093/bioinformatics/8.3.275.

C.I. Keeling, J. Bohlmann, Genes, enzymes and chemicals of terpenoid diversity in the constitutive and induced defence of conifers against insects and pathogens, New Phytol. 170 (2006a) 657–675, https://doi.org/10.1111/j.1469-8137.2006.01716.x.

C.I. Keeling, J. Bohlmann, Diterpene resin acids in conifers, Phytochemistry 67 (2006b) 2415–2423, https://doi.org/10.1016/j.phytochem.2006.08.019.

T.G. Köllner, M. Held, C. Lenk, I. Hiltpold, T.C.J. Turlings, J. Gershenzon, J. Degenhardt, A maize (*E*)-β-caryophyllene synthase implicated in indirect defense responses against herbivores is not expressed in most American maize varieties, Plant Cell 20 (2008) 482–494, https://doi.org/10.1105/tpc.107.051672.

J.-W. de Kraker, M.C.R. Franssen, A. de Groot, W.A. König, H.J. Bouwmeester, (+)-Germacrene A biosynthesis: the committed step in the biosynthesis of bitter sesquiterpene lactones in chicory, Plant Physiol. 117 (1998) 1381–1392, https://doi.org/10.1104/pp.117.4.1381.

S. Kumar, G. Stecher, K. Tamura, MEGA7: Molecular evolutionary genetics analysis version 7.0 for bigger datasets, Mol. Biol. Evol. 33 (2016) 1870–1874, https://doi.org/10.1093/molbev/msw054.

P.-M. Kuo, K.-H. Hsu, Y.-R. Lee, F.-H. Chu, S.-Y. Wang, Isolation and characterization of β-cadinene synthase cDNA from *Chamaecyparis formosensis* Matsum, Holzforschung 66 (2012) 569–576, https://doi.org/10.1515/hf-2011-0224.

Y.-H. Kuo, L.-L. Shiu, Two new sesquiterpenes, 12-hydroxy-α-longipinene and 15-hydroxyacora-4(14), 8-diene, from the heartwood of *Juniperus chinensis* LINN. var. *tsukusiensis* MASAM, Chem. Pharm. Bull. 44 (1996) 1758–1760, https://doi.org/10.1248/cpb.44.1758.

D. Liang, W. Li, X. Yan, Q. Caiyin, G. Zhao, J. Qiao, Molecular and functional evolution of the spermatophyte sesquiterpene synthases, Int. J. Mol. Sci. 22 (2021) 6348, https://doi.org/10.3390/ijms22126348.

T.-C. Lin, J.-M. Fang, Y.-S. Cheng, Terpenes and lignans from leaves of *Chamaecyparis formosensis*, Phytochemistry 51 (1999) 793–801, https://doi.org/10.1016/S0031-9422(99)00074-6.

L.-T. Ma, Y.-R. Lee, P.-L. Liu, Y.-T. Cheng, T.-F. Shiu, N.-W. Tsao, S.-Y. Wang, F.-H. Chu, Phylogenetically distant group of terpene synthases participates in cadinene and cedrane-type sesquiterpenes accumulation in *Taiwania cryptomerioides*, Plant Sci. 289 (2019), 110277, https://doi.org/10.1016/j.plantsci.2019.110277.

L.-T. Ma, C.-H. Wang, C.-Y. Hon, Y.-R. Lee, F.-H. Chu, Discovery and characterization of diterpene synthases in *Chamaecyparis formosensis* Matsum. which participated in an unprecedented diterpenoid biosynthesis route in conifer, Plant Sci. 304 (2021), 110790, https://doi.org/10.1016/j.plantsci.2020.110790.

F.A. Macías, J.M.G. Molinillo, R.M. Varela, J.C.G. Galindo, Allelopathy–a natural alternative for weed control, Pest Manag. Sci. 63 (2007) 327–348, https://doi.org/10.1002/ps.1342.

D.M. Martin, J. Fäldt, J. Bohlmann, Functional characterization of nine Norway Spruce TPS genes and evolution of gymnosperm terpene synthases of the TPS-d subfamily, Plant Physiol. 135 (2004) 1908–1927, https://doi.org/10.1104/pp.104.042028.

R.P. McAndrew, P.P. Peralta-Yahya, A. DeGiovanni, J.H. Pereira, M.Z. Hadi, J. D. Keasling, P.D. Adams, Structure of a three-domain sesquiterpene synthase: a prospective target for advanced biofuels production, Structure 19 (2011) 1876–1884, https://doi.org/10.1016/j.str.2011.09.013.

S.R. Meshnick, Artemisinin: mechanisms of action, resistance and toxicity, Int. J. Parasitol. 32 (2002) 1655–1660, https://doi.org/10.1016/s0020-7519(02)00194-7.

A. Mithöfer, W. Boland, Plant defense against herbivores: chemical aspects, Annu. Rev. Plant Biol. 63 (2012) 431–450, https://doi.org/10.1146/annurev-arplant-042110-103854.

M. Mizutani, F. Sato, Unusual P450 reactions in plant secondary metabolism, Arch. Biochem. Biophys. 507 (2011) 194–203, https://doi.org/10.1016/j.abb.2010.09.026.

D.A. Nagegowda, M. Gutensohn, C.G. Wilkerson, N. Dudareva, Two nearly identical terpene synthases catalyze the formation of nerolidol and linalool in snapdragon flowers, Plant J. 55 (2008) 224–239, https://doi.org/10.1111/j.1365-313X.2008.03496.x.

E. Pichersky, E. Lewinsohn, Convergent evolution in plant specialized metabolism, Annu. Rev. Plant Biol. 62 (2011) 549–566, https://doi.org/10.1146/annurev-arplant-042110-103814.

K.A. Rising, C.M. Starks, J.P. Noel, J. Chappell, Demonstration of germacrene A as an intermediate in 5-epi-aristolochene synthase catalysis, J. Am. Chem. Soc. 122 (2000) 1861–1866, https://doi.org/10.1021/ja993584h.

E. Sharma, G. Anand, R. Kapoor, Terpenoids in plant and arbuscular mycorrhiza-reinforced defence against herbivorous insects, Ann. Bot. 119 (2017) 791–801, https://doi.org/10.1093/aob/mcw263.

C.M. Starks, K. Back, J. Chappell, J.P. Noel, Structural basis for cyclic terpene biosynthesis by tobacco 5-epi-aristolochene synthase, Science 277 (1997) 1815–1820, https://doi.org/10.1126/science.277.5333.1815.

Y.-C. Su, C.-L. Ho, E.I.-C. Wang, Analysis of leaf essential oils from the indigenous five conifers of Taiwan, Flavour Fragr. J. 21 (2006) 447–452, https://doi.org/10.1002/ffj.1685.

S.-Y. Wang, C.-L. Wu, F.-H. Chu, S.-C. Chien, Y.-H. Kuo, L.-F. Shyur, S.-T. Chang, Chemical composition and antifungal activity of essential oil isolated from *Chamaecyparis formosensis* Matsum. wood, Holzforschung 59 (2005) 295–299, https://doi.org/10.1515/HF.2005.049.

Y. Yoshikuni, T.E. Ferrin, J.D. Keasling, Designed divergent evolution of enzyme function, Nature 440 (2006) 1078–1082, https://doi.org/10.1038/nature04607.